Limitations in the application of computer simulations of temperature rise of completely new designs of MV metal enclosed switchgear

Elin Fjeld, *Member*, *IEEE*, Atle Pedersen, Martin Kriegel, Shailendra Singh, Sergio Barrio, Jaroslav Snajdr, and ZuHui Li

***Abstract*—Temperature rise simulation deals with different physical domains describing heat generation and heat dissipation effects. Cigré working group A3.36 has conducted a study on temperature rise simulation of switchgear for distribution and transmission level. The working group built up new, manufacturer independent devices. Members of the working group simulated the temperature rise in advance to the tests, which were performed at laboratories of universities, as independent parties. In order to assess the simulation accuracy, the simulation results are compared to each other and to the measured results. This paper summarizes the main findings from the medium voltage device. The study has shown that when simulating the temperature rise on a completely new design, with reliable input values of contact resistances and emissivity coefficients, an accuracy of about 25 % could be expected. Primary reason seems to be based on the complexity of simulating the heat dissipation mechanisms. To get a more accurate result, verification and validation is needed in order to adjust the parameters determining the heat dissipation. This study has also illustrated that it requires good knowledge (especially of the radiation) in order to adjust these parameters properly.**

***Index Terms*— CFD, MV switchgear, Temperature Rise Simulation, Temperature Rise Test, Thermal Network Method.**

I. Introduction

The development of medium voltage (MV) and high voltage (HV) switchgear comes along with a bundle of simulation and testing tasks to ensure a safe and reliable operation of the equipment over several decades. During normal operation as well as in case of short-circuit events the temperature inside the switchgear rises above ambient level. To prevent accelerated ageing of the equipment, temperature rise limits are given in the standards, depending on the used insulating media [1]. The optimization of existing as well as the development of future switchgear require the knowledge to predict the temperature rise of the equipment during the different iterations of the development process.

Simulation of the temperature rise of a switchgear can be divided in the following categories: Simplified methods, Thermal Network Method (TNM) and the finite elements method / CFD. These methods are usually used in the different design process phases. (i.e. simplified methods as first approximation for quotation and TNM and CFD during the design of the equipment). In addition, these methods are also used together, see e.g. [2].

Simplified methods, as e.g. reported in [3], will normally focus on getting a fast, rough first estimate of the temperature of the most critical parts. To get a more detailed picture of the temperature distributions, TNM or CFD will typically be applied. In the literature, the reported accuracy of these methods can be as good as ±2-5 K, see e.g. [4-7]. The high accuracies reported are typically found after model calibration, i.e. when the simulations are performed with some experimental results available on similar designs as initial calibration point or as knowledge of the user.

However, in case of a completely new switchgear design (unknown test response), there will be some uncertainty in the input parameters, and a simulation cannot be more accurate than the input parameters. The goal of this study is to assess the predictive power of simulation tools for not yet experimentally characterized switchgear. The result from the HV switchgear, is previously published in [8]. It shows that reliable simulation of the power input, require knowledge of the overall resistance along the current path. Estimations based on the individual contact resistances tend to overestimate the contribution from contact resistances. Further, it is shown that even with a good estimate of the power input the simulated temperature rises could vary significantly due to different modelling of heat dissipation mechanisms. The conclusion is that temperature rise simulations can only be reliable when a similar reference case is available for adjusting the heat dissipation simulation.

This paper presents the results for the MV switchgear. In this case more input parameters, such as measured resistance and emissivity, were available before simulation, and a better accuracy of the power loss simulations were expected. As for the HV device, the test was performed as a blind test, meaning that no experimental temperature results were available before the simulation.

After the comparison between simulation and test results for the MV device, one member of the working group verified and validated his simulation tool to the first test result. Then the test current and the emissivity of the current path was changed and

This work performed by the Cigré working group A3.36. E. Fjeld is with Department of Electrical Engineering, IT and Cybernetics, University of South-Eastern Norway, Porsgrunn (e-mail: elin.fjeld@usn.no). A. Pedersen is with SINTEF Energy AS, Trondheim, Norway (e-mail: atle.pedersen@sintef.no). M. Kriegel is with ABB Power Grids Switzerland Ltd, Zurich (e-mail: martin.kriegel@ch.abb.com). S. Singh is with ABB AS, Electrification – Distribution solutions, Skien, Norway (e-mail: shailendra.singh@no.abb.com). S. Barrio is with Ormazabal Corporate Technology, Amorebieta, Bizkaia, Spain (e-mail: sbr@ormazabal.com). Jaroslav Snaidr is with Schneider Electric, Regensburg, Germany (e-mail: jaroslav.snaidr@se.com). ZuHui Li is with Eaton Electrical Ltd., Suzhou, China (e-mail: zuhuili@eaton.com).

the influence on the test results was studied together with how well the simulation was able to reflect these changes.

II. Theory

The temperature rise is a balance between the heat generation and heat dissipation.

A. Heat generation

If external heat sources (as sun radiation) are not considered, the main heat source is the ohmic losses of the current path. This power loss, *P*, is given by:

$$P = RI_r^2 \tag{1}$$

where *R* is the resistance of the current path and I_r is the current. The resistance along the current path consists of the bulk resistance of the conductors (R_{bulk}) and the contact resistance (R_{cont}) of the connections between different conductors:

$$R = R_{bulk} + R_{cont} \tag{2}$$

In addition, losses may occur in magnetic steel near the current path (enclosure, screws, nuts, bushings etc.) due to Eddy-currents and hysteresis losses. These effects may eventually be reduced or eliminated by proper design or by using nonmagnetic materials.

The resistance of the conductor increases with temperature. The resistance during load conditions, can be calculated according to

$$R_{bulk} = \rho \frac{l}{A_{cs}}(1 + \alpha \Delta T) \tag{3}$$

where ρ is the specific resistance at reference conditions, A_{cs} is the cross-sectional area of the conductor material, α is the temperature coefficient, and ΔT is the temperature difference of the conductor between reference and load conditions. Under AC load, the effective cross-sectional area might be significantly reduced due to skin and proximity effects, see e.g. [6].

The contact resistance is due to the constriction of the current when passing from one contact member to the next, because the conductors only have metallic contact in small spots, called a-spots [9]. The contact area depends on the applied pressure, the surface state of the contacts, and the hardness of the material used, and the contact resistance will thus depend on the rated current and the contact design.

For stationary connections (bolted, welded, soldered, pressed) a high force may be applied. Switching equipment requires the use of a movable (open/close, sliding or rotating) contact. When designing these contacts, there will be a tradeoff between contact force and friction (mechanical energy of the drive for vacuum interrupter contacts). The movable contacts will thus typically have somewhat higher contact resistances compared to the stationary contacts. Typical values may vary in the range 0.1 – 10 μΩ.

B. Heat dissipation

The generated heat can be transferred to a place of lower temperature by three different mechanisms (usually occurring together); thermal conduction, convection and radiation.

Conductive heat transfer is energy transport due to molecular motion and interaction. The power conducted through a cross-sectional area A_{cs} is given by Fourier's law

$$P_{cond} = -kA_{cs}\nabla T \tag{4}$$

where k is the thermal conductivity of the material and ∇T is the temperature gradient. With solids, the thermal conductivity generally does not vary much with temperature; in the case of liquids and gases, on the other hand, it is often strongly influenced by temperature. For many simple applications, only heat conduction in one dimension needs to be considered, and the temperature gradient might be replaced by e.g. $\frac{dT}{dx}$ for conduction along the *x*-direction.

Convective heat transfer is energy transport due to bulk fluid motion. Convection heat transfer through gases and liquids from a solid boundary results from the fluid motion along the surface. Newton's law gives the power transferred by convection

$$P_{conv} = hA_{surf}(T_s - T_0) \tag{5}$$

where A_{surf} and T_s are the surface area and temperature of the hot surface, respectively, h is the heat transfer coefficient, and T_0 is the temperature of the surrounding fluid. The heat transfer coefficient depends on the type of fluid, the fluid velocity, the temperature and forced vs free convection. For natural convection, the value of h is typically between 5 – 10 W/m^{2}K for large surfaces in air. The gas flow can be made more intense by applying for example a fan, known as forced convection. Forced convection, typically results in a substantial increase in the heat transfer capacity. For actual switchgear, the gas flow and the heat transfer coefficient may be different for different parts.

Radiative heat transfer is energy transport due to emission and absorption of electromagnetic waves or photons from a surface or volume. The radiation does not require a heat transfer medium and can occur in vacuum. The power radiated from a hot surface with absolute temperature T_s to a much larger, surrounding surface with a colder surface of temperature T_0, is given by

$$P_{rad} = f_{view}\varepsilon\sigma_s A_{surf}(T_s^4 - T_0^4) \tag{6}$$

where A_{surf} is the surface area emitting the radiation and σ_s is Stefan-Boltzman constant ($5.67 \cdot 10^{-8}$ W/m^{2}K^4). ε is the emissivity of the surface (value between 0 and 1), and depends on many effects (surface treatment, oxidation) and may change with time. f_{view} is a geometric factor or view factor (≤1) to account for the radiation exchange with other hot surfaces.

Fig. 1 indicates the heat transfer mechanisms involved for a medium voltage metal enclosed switchgear without ventilation openings.

This article has been accepted for publication in a future issue of this journal, but has not been fully edited. Content may change prior to final publication. Citation information: DOI 10.1109/TPWRD.2020.3026074, IEEE Transactions on Power Delivery

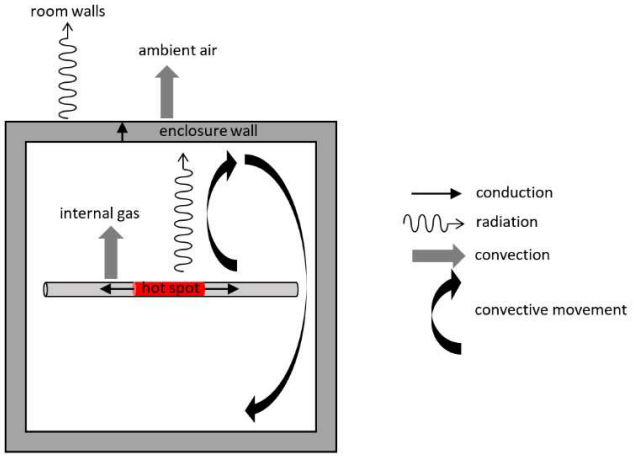

Fig. 1. *Heat transfer mechanisms inside and outside a metal enclosed switchgear (without ventilation openings).*

First, the heat transfer inside the enclosure is considered. Heat is transferred by conduction from the hot spots (e.g. contacts) to cooler parts of the current path (e.g. busbars and cables). Thus, the conduction contributes to even out the temperature differences along the current path. The gas inside the switchgear is heated due to convective heat exchange with the current path. Buoyancy causes convective movement of the internal gas, which transfers heat to the inner walls of the enclosure. In addition, all parts inside the enclosure with an overtemperature (relative to the enclosure walls) will transfer energy to the inner walls of the enclosure by radiation. The process of heat exchange becomes even more complex if parts of the current path are covered by various construction elements. Such construction elements may restrict the convection and radiation from the hot spots. However, the effect might be compensated by heat conduction to a larger heat exchange surface.

Second, the heat transfer from the enclosure to the ambient has to be considered. The heat is transported by conduction across the enclosure walls. If the enclosure is hermetically sealed, cooling of the enclosure can only be achieved by heat transfer from the outer walls to the surroundings by radiation and convection, as shown in Fig. 1.

C. Thermal Network Model (TNM)

The Thermal Network Model (TNM) is based on a substitution of a 3D geometry by an equivalent thermal circuit consisting of thermal resistances, capacitances and heat sources. The temperatures are calculated at the connection point of the thermal elements (resistances, heat sources etc) of this equivalent network. The mathematical formulation of a thermal circuit problem is similar to an electrical circuit and can be solved by electrical network analysis tools.

In general, a thermal network method is based on nodal analysis where each node represents a part of a studied system, typically a segment of a copper bar, a heatsink or a gas environment. This node is then described by mathematical equations according to its connections to neighboring nodes and its properties and sources. The connections represent individual heat transfer principles of conduction, convection and radiation and they are described by appropriate formulas expressing thermal resistance. The parameter set (dissipation) is explicitly fixed by the user/software (convective heat transfer coefficient, areas, view factor etc.) based on geometric features, pre-existing empirical relation etc. The heat sources (generation) due to current flow are the inputs of the problem and are specifically entered for each source element (bulk and contact resistance).

Once preprocessing part is finished and the studied system is created, a solver based on Kirchhoff's circuit laws (e.g. a network solver like PSpice) transforms all the relations between nodes into a matrix and iterates the solution unless the sum of incoming and out coming flows in all the nodes is zero, resulting in a temperature distribution at all the nodes.

D. Computational Fluid Dynamics (CFD)

CFD is defined as discretized methods for partial differential equations (PDE), solved numerically by methods such as Finite Element, Finite Volume or Finite Difference Methods. The fundamental basis of almost all CFD problems is the Navier–Stokes equations describing the fluid flow. CFD is solving the advection diffusion equation in the context of fluid or fluid solid interface. Even in pure flow field where the velocity of the flow is zero, heat transfer in fluid can happen with conduction or diffusion. For solids in the models, the same general form of equation has been solved by making the velocity component zero. Thus, the same solver algorithm has been applied to solve all the equations.

The preparation of the geometry for a CFD analysis is typically done via a CAD tool. It is critical to determine the level of details which is required for properly representing the problem to be solved. In case for a switchgear it may be necessary to neglect bolts and nuts, simplify contacts etc. Otherwise the spatial discretization will become huge and computational resources might not be available to achieve a solution within a reasonable time.

The location of the domain boundaries (i.e. initial pressure, temperature, velocity, currents etc.) is applied during the preprocessing together with heat generation sources. The dissipation parameters (convective heat transfer coefficient, areas, view factor etc.) are implicitly fixed based on the material properties, geometry etc.

During the mesh generation, the domain is discretized into much smaller volumes and the PDEs are converted into discrete algebraic equations over the mesh. The next phase is solving these algebraic equations. The equation system can be solved using either direct or iterative solvers. A direct solver finds a solution of the system of algebraic equations by Gauss elimination or matrix inversion. An iterative solver starts by assuming an approximate solution for the unknowns. The solution is iterated until the convergence criteria is reached. In the end, the variables (pressure, velocity, temperature etc) are calculated at the element nodes/control volume and interpolated in-between.

III. Test Device

The MV test device was set up by the working group. Instead of taking an existing product, the device was designed by the working group to be manufacturer-independent. Thus, the performance of the device was unknown to all members. Sharing of the drawings was easy as no restriction (e.g. NDA) needed to be considered.

The MV device is a stainless steel tank with volume corresponding to an SF_6-filled 12/24 kV switchgear, see Fig. 2. The testing and simulation were performed with air at atmospheric pressure as the insulating gas.

Fig. 2. Medium voltage test device. The enclosure corresponds to an SF_6-filled 12/24 kV switchgear. The device was connected with the three phases on one side and the other side short circuited.

The unit consisted of three modules. The two outer modules were designed to represent the cable modules, with a knife-blade load break switch (LBS). Due to a limited number of switches available, only one phase (L1) was equipped with switches in both modules. The two other phases were equipped with one switch and one "replacement bar", see Fig. 3.

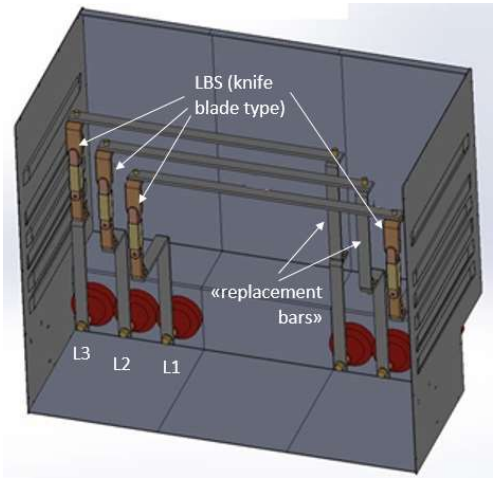

Fig. 3. Inside view of the test device. Phase L1 was equipped with a load break switch (LBS) in each cable module, while the other phases were equipped with one LBS and one "replacement bar".

The center module of the test object (typically the transformer T-off equipped with a vacuum circuit breaker or a LBS in combination with HV fuses) was empty, and the current was passing from one cable module via the busbars through the second cable module. This is the normal path for the main current through the switchgear during normal conditions in a common cable ring distribution system. Simplified heat transfer calculations as described in [3] was used to find appropriate cross-sections of the conductors in order to get a temperature rise in a realistic range (i.e. close to the IEC limits [1]). The cross-section of the conductors (except the LBS) was 40x6mm^2.

The device was connected with the three phases on one side and the other side short circuited, as seen in Fig. 2.

The different parts of the current path were either bare copper conductors or silver-coated copper. The top and rear surface (inner and outer) of the enclosure was painted black. The emissivity coefficients for the conductors and steel enclosure were measured. The results are given in TABLE 1 and was available before the simulation.

TABLE 1
Measured emissivity (ε) for the conductors and the enclosure.

	ε
Unpainted steel enclosure surfaces	0.4
Black painted steel enclosure surfaces	0.9-1
Bare copper conductors	0.2-0.3
Silver-coated copper conductors	0.1-0.2

In addition, the resistance at room temperature was measured with 100 A DC and provided to the group members prior to the simulation. The total resistance per phase bushing to bushing (inside the enclosure) after one heat run is given in TABLE 2. The contact resistances of the movable contacts (rotating and open/close contacts) were found to be very sensitive to small movements. Average measured values were thus given in accordance with TABLE 3.

TABLE 2
Total resistance per phase measured with 100 A DC from bushing to bushing (inside the enclosure).

Phase	R_{tot} [μΩ]
L1	195
L2	162
L3	158

TABLE 3
Average contact resistance measured with 100 A DC.

Type of contact	R_{cont} [μΩ]
Bolted connection	2.5
Rotating contact	16
Open/close contact	11

IV. Temperature Rise Test

The switchgear was operated with air at atmospheric pressure. The partially sealed enclosure was without any ventilation during the measurements. Thermal testing was carried out with a three-phase current of 630 A, at a frequency of 50 Hz, supplied from a high current injector test equipment (Hilkar type AK23). The temperature rise was logged until all sensors showed that steady state conditions (< 1 K/hour) were reached. This took approximately 4.5 hours. The ambient/room temperature at steady state was 22 ºC.

The temperature was measured by thermocouples (type K). The temperature rise along the current path in phase L1 is shown by the dotted line in Fig. 4. It can be seen that the temperature rise was around 90 K, i.e. higher than the allowable temperature rises according to IEC (75 K). However, the aim of this tests was not to fulfil IEC standards, but provide a

This article has been accepted for publication in a future issue of this journal, but has not been fully edited. Content may change prior to final publication. Citation information: DOI 10.1109/TPWRD.2020.3026074, IEEE Transactions on Power Delivery

representative test object with temperature rise in the relevant range.

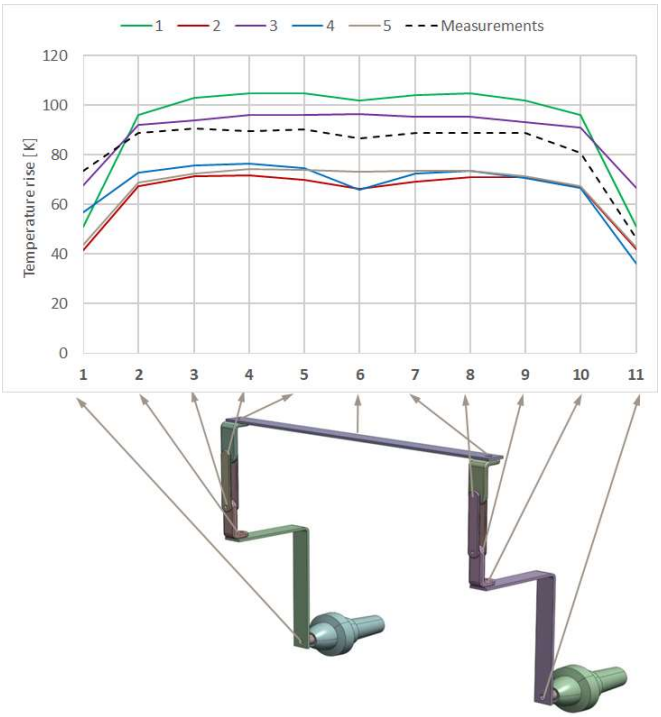

Fig. 4. Measured (dotted line) and simulated (solid lines) temperature rise along the current path of phase L1. The curve numbers (1-5) are the five simulation results. Simulation no 4 is performed with TNM, while the rest are with CFD. The numbers on the horizontal axis (1-11) represents the temperature sensor locations.

V. Simulations

Five members of the working group simulated the temperature rise for the MV test device, using either CFD-simulation or thermal network model. The simulation was performed as a "blind test", i.e. the measured temperature rise was not known prior to the simulation.

The users were given the 3D drawings, measured emissivities and resistance at room temperature and the test conditions (ambient temperature, load current, filling gas and pressure). It was up to the person performing the simulation how to implement the input parameters, choose appropriate values for other, unknown parameters, and to decide how to consider the boundary conditions based on previous experience and knowledge. This might be the normal procedure in case of a completely new design with unknown test response.

Fig. 5 shows typical results from temperature rise simulation. It can be seen that the hottest spots are, as expected, at the switches in phase L1 (the phase containing two LBSs).

Eleven temperature evaluation points were defined along the current path of phase L1, as seen in Fig. 4. At those points the calculated temperature is compared against other simulations as well as against test result. The results from the different simulations are shown in Fig. 4. The estimated temperature rises of the hottest spot (sensor 8) was in the range 78 – 105 K. Compared with the measured value of 90 K, this gives a deviation of up to 25 %.

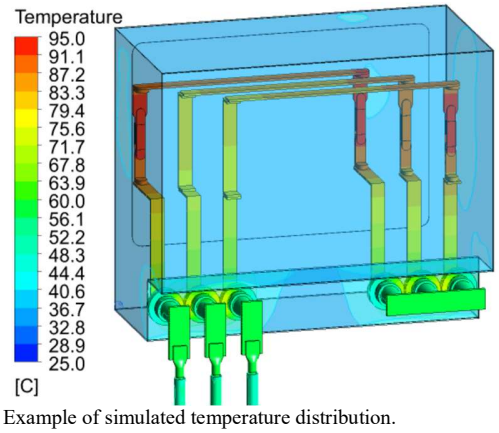

Fig. 5. Example of simulated temperature distribution.

The results indicate that for a completely new switchgear design, the accuracy of the temperature rise estimation is probably more dependent on the user's experience in selecting the proper input parameters and necessary simplifications, rather than what kind of simulation tool (CFD or TNM) is applied. A detailed comparison of the different approaches is therefore out of the scope for this paper, and in the following analysis, the focus will be on the accuracy of the estimated power input and the heat dissipation simulation.

A. Accuracy of estimated power input

In this study the average contact resistance and the overall resistance at room temperature were given before simulations, and a better estimation of the power input was assumed compared to the HV study [8]. However, for the MV device, the simulated power loss varied from 240 to 340 W. The reason for the variation might be different material properties, different ways of distributing the contact resistances or different methods to consider the temperature dependency of the resistance. Another reason can be different methods to include AC-losses, such as skin effect, proximity effect and simulation of losses in the enclosure.

Simplified estimations of the power losses according to [3] give a power loss around 260 W. Experience on a similar device, with direct power measurements with a wattmeter, have shown insignificant contribution from AC-losses [10]. Based on this, one can assume that the power losses in the upper range (above 300 W) are most probably over estimated.

B. Accuracy of heat dissipation simulation

Fig. 6 shows the maximum simulated temperature rise (at sensor 5, open/close contact) over the total simulated power loss for the five simulations. As seen from the figure, there is no proportionality between the losses and temperature rise.

Simulation no 1 and 2 have almost the same power loss estimate, while the maximum temperature rise deviates by 37 K. Based on this, it is assumed that the high discrepancy

The highest discrepancy between the simulated and measured temperature rise was up to 25 % in this study. Based on Fig. 6, it this difference is assumed to be mainly due to different simulation of the heat dissipation.

One of the simulation with best power loss estimation (270 W) has the largest deviation between simulated and measured temperature rise (the measured temperature rise was 90 K).

This shows that the different members use different heat dissipation models.

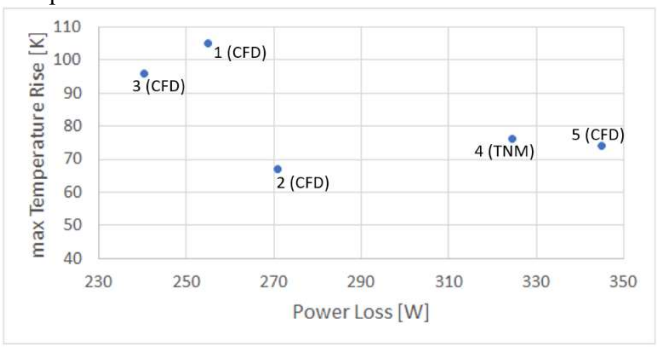

Fig. 6. Maximum simulated temperature rise vs simulated power loss. The simulation number (1-5 from Fig. 4) is indicated together with the simulation tool applied.

The highest discrepancy between the simulated and measured temperature rise was up to 25 % in this study. Based on Fig. 6, it this difference is assumed to be mainly due to different simulation of the heat dissipation.

The accuracy of this study is around 25 % compared to the measurement, mainly due to different simulation of the heat dissipation. It should be noted that the test device is a simplified design compared to a real switchgear. I.e. there were no conductors in the middle module and no structures needed to keep the current path stable or to operate the switching devices. These elements might complicate the heat dissipation simulation as they might function as local heat sinks and might affect the view factor for the radiation in (6). Simulating the heat dissipation mechanisms for a real device is thus expected to be more challenging than for this test device.

To achieve higher accuracy, experience or experimental results from a similar device is required in order to adjust the heat transfer simulation. If this is available, the accuracy of further estimates will depend on whether the correct parameters are adjusted. In the following section, the measurements results have been provided to one of the group members. The member was then given the opportunity to adjust the initial simulation (thermal network model) to fit with the measured temperature rise. Then some test parameters are changed to see how well the simulation can predict the new temperature rise.

VI. Changing the Test Parameters

The final temperature rise of the switchgear depends on the efficiency of the three heat dissipation mechanisms; radiation, convection and conduction. Eq. (5) shows that the convection depends linearly on the temperature difference between the conductor and the surrounding gas, through the heat transfer coefficient. The radiated power is given by (6) and depends on the surface emissivity and the absolute temperature to the fourth power, which means that the portion of radiation will increase with increasing temperature. Including radiation in the simulations complicates the model as it brings in a yet another reference temperature, namely the wall temperature of the enclosure. In addition, it depends on the surrounding elements (included in the view factor).

In this section, the temperature rise is studied with varying the temperature range and the emissivity of the conductors. Temperature rise tests are performed with different load currents: 630 A, 500 A, 400 A, 200 A. The different load currents will represent different temperature ranges.

First the temperature rise tests were performed with the original surface of the conductors, see Fig. 7(a), i.e. with an emissivity around 0.2 (ref TABLE 1). Then the conductors were painted with matt, black paint, see Fig. 7(b), which gave an emissivity close to 1, and the tests were repeated. Increasing the emissivity values to up to 1 can be regarded as an extreme case, but (in an oxidizing environment) the emissivity of the conductors will increase as oxidation processes take place and the emissivity may increase up to 0.65. This oxidation is relevant for AIS, but SF_6 GIS will not undergo oxidation of conductors inside the tank.

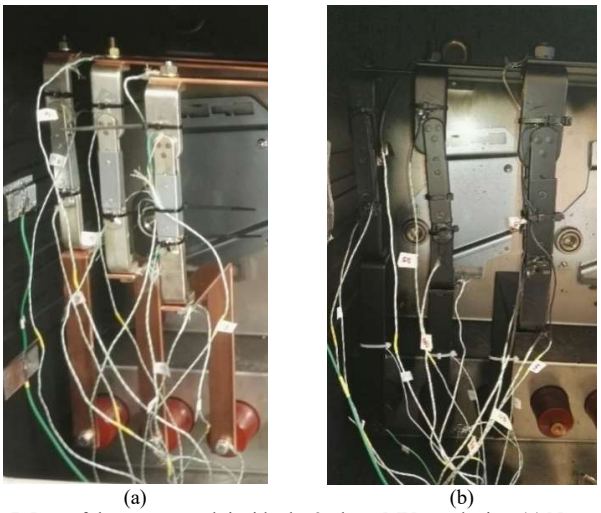

(a) (b)

Fig. 7. Part of the current path inside the 3-phase MV test device. (a) Not painted. (b) Painted with matt, black paint.

A. Changing the temperature range (load currents)

Fig. 8 shows the measured and simulated temperature rise for the open/close contact in phase L1 for different load currents. The simulation was done with a thermal network model using Boltzmann law, as given by (6), to consider radiation. It can be seen that even though the simulation is adjusted to fit the 630 A case, a deviation of about 10 K is found when reducing the load current to 500 A. Most likely this is due to the choice of values for the variables of equation (6); emissivity, view factor or surface area. The percentage deviation between measurements and simulation increases with reducing temperature/load current.

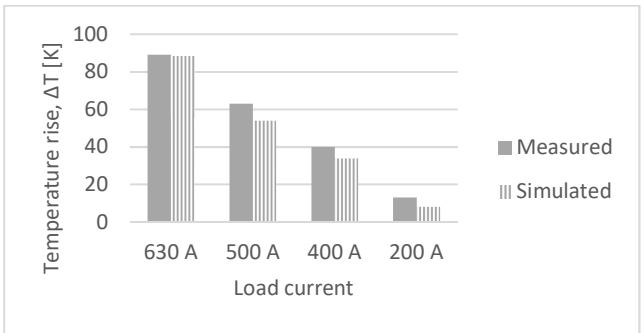

Fig. 8. Measured and simulated temperature rise of the open/close contact (sensor 8) for different test currents for unpainted conductors. For the test current of 630 A, the simulations were adjusted to fit the measurements. The simulation was used to predict the temperature rise for new test current.

B. Changing the emissivity coefficients

When the conductors were painted black, the measured temperature rise was lowered by 20-25 %. The result for the load current of 630 A is given in Fig. 9 together with the corresponding simulation result. It can be seen that also here, the simulation deviated by 10 K, again indicating that this is mainly caused by accuracy of modelling radiation rather than other heat dissipation effects.

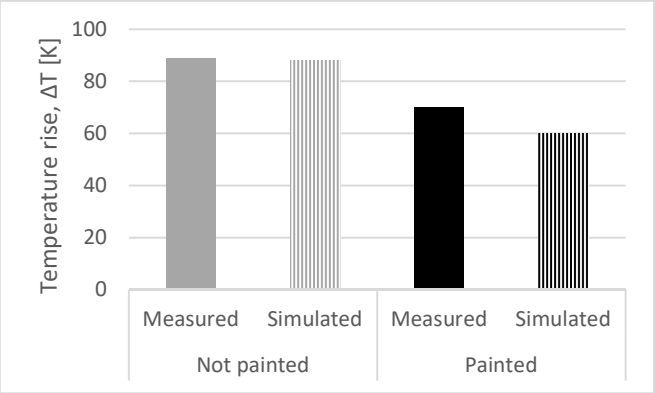

Fig. 9. Measured and simulated temperature rise of the open/close contact (sensor no 8) with a test current of 630 A for not painted and painted conductors. The simulations were adjusted to fit the measurements for the not painted case. Then, the simulation was used to predict the temperature rise when the conductors were painted.

In both cases, the simulated temperature rise is lower than the actual measured temperatures. This implies that the simulation over-estimate the contribution from radiation. The results show that including radiative heat transfer in the simulation will increase the complexity of the model, and the user of the simulation tool need to have good experience in order to tune the parameters properly.

Based on the measurements, rough estimates could be made for the portion of power dissipation by radiation. The results for the 500 A and 200 A case are given in TABLE 4. For the non-painted conductors (with emissivity around 0.2), it was found that about 10 % of the power loss was transferred by radiation at around 30 °C absolute temperature (200 A case). When the absolute temperature was around 70 – 80 °C i.e. near the IEC limits (500 A case), the portion of radiation was increased to about 20 %. For the painted conductors (with emissivity around 1), it was found that about 40 % of the power loss was dissipated by radiation at around 30 °C absolute temperature (200 A case). When the absolute temperature was around 80 °C (500 A case), the portion of radiation was increased to about 50 %. It is clear that in order to simulate the temperature rise with a certain accuracy, the radiation needs to be included, at least for temperatures in the relevant temperature range (close to the IEC).

TABLE 4
Estimated portions of power loss by radiation for different emissivity values and temperature ranges.

T [°C]	P_{rad}/P_{tot}	
	$\varepsilon \approx 0.2$	$\varepsilon \approx 1$
70-80	20 %	50 %
30-35	10 %	40 %

VII. Conclusion

This study has shown that when simulating the temperature rise on a completely new design, with reliable input values of contact resistances and emissivity coefficients, an accuracy of about 25 % could be expected, independent on the simulation tool. Primary reason seems to be based on the complexity of simulating the heat dissipation mechanisms. To get a more accurate result, verification and validation is needed in order to adjust the parameters determining the heat dissipation. This study has also illustrated that it requires good knowledge (especially of the radiation) in order to adjust these parameters properly.

VIII. Acknowledgment

The authors gratefully acknowledge the contribution from Dr. Jakub Korbel during the simulation part of this work.

IX. References

[1] IEC Standard 62271-1: High-voltage switchgear and controlgear – Part 1: Common specifications for alternating current switchgear and controlgear, ed.2.0, 2017.

[2] S. Singh, R. Summer and U. Kaltenborn “A Novel Approach for the Thermal Analysis of Air Insulated Switchgear”, in Proc. CIRED Conference, Frankfurt, 2011, paper no 0429.

[3] E. Fjeld, W. Rondeel, E. Attar and S. Singh, “Estimate the Temperature Rise of Medium Voltage Metal Enclosed Switchgear by Simplified Heat Transfer Calculations”, *IEEE Trans. On Power Delivery*, accepted May 2020.

[4] S. Pawar, K. Joshi, L. Andrews and S. Kale, "Application of Computational Fluid Dynamics to Reduce the New Product Development Cycle Time of the SF_6 Gas Circuit Breaker", IEEE Trans. on Power Delivery, vol. 27, no. 1, pp.156-163, Jan. 2012.

[5] H. Song, G. Hou, W. Wang, X. Deng, Q. Huang, W. Mo, M. Hasegawa and X. Li., "Application of computational fluid dynamics to predict the temperature-rise of gas insulated switchgears," ICEPE-ST, Xi'an, 2017, pp. 694-697.

[6] X. Dong, R. Summer and U. Kaltenborn, “Thermal Network Analysis in MV Design”, in Proc. CIRED Conference, Prague, 2009, paper no 0637.

[7] M. T. Dhotre, J. Korbel, X. Ye, J. Ostrowski, S. Kotilainen and M. Kriegel, “CFD Simulation of Temperature Rise in High-Voltage Circuit Breakers”, *IEEE Trans. On Power Delivery*, vol. 32, no. 6, pp. 2530-2536, Dec. 2017.

[8] M. Kriegel, E. Fjeld, A. Pedersen, P. G. Nikolic, T. Krampert, J. Snajdr, “Benchmark Case of Multiphysics Simulation for Temperature Rise Calculation”, in *Proc. Int. Conf. on Condition Monitoring, Diagnosis and Maintenance* (CMDM), pp. 93-100, Bucharest, Romania, Sept. 2019.

[9] R. Holm, “Electrical Contact Resistance: Fundamental Principles”, in *Electric Contacts. Theory and Applications*, Springer-Verlag, Berlin, Germany, 1967.

[10] E. Fjeld, W. Rondeel, K. Vaagsaether, M. Saxegaard, P. Skryten, E. Attar, “Thermal Design of Future Medium Voltage Switchgear”, in Proc. CIRED Conference, Lyon, 2015, paper no 1090.

X. Biographies

Elin Fjeld (M’14) received the M.S. degree in applied physics from the Norwegian University of Science and Technology (NTNU), Trondheim, in 2007, and Ph.D. degree in electrical power engineering from University of South-Eastern Norway (USN), Porsgrunn, in 2014.

Her employment experience includes Researcher at the Norwegian Defense Research Establishment and Postdoctoral Fellow at USN. Currently, she is working as an Associate Professor at USN.

Atle Pedersen received the M.Sc. degree and the PhD degree in electrical power engineering from the Norwegian University of Science and Technology (NTNU), Trondheim, Norway in 1994 and 2008 respectively.

He has worked at ABB Distribusjon in Skien Norway from 1994 – 2001. He has been in SINTEF Energy Research since 2006. His field of interest include HV switchgear, power cables, and testing of HV apparatus. His research work also includes dielectric, electromagnetic and electro thermal simulations of power devices.

Martin Kriegel received the Ph.D. degree in electrical engineering from the Institute for High Voltage Technology, RWTH, Aachen, Germany in 1998.

He has since worked for ABB, Baden, Switzerland, in various position and locations in research and development. He is currently working as Senior Principal Engineer for the development of high voltage circuit breakers. He is member of IEC and has been active in Cigré working groups that deal with simulation as verification tools.

Shailendra Singh received the B.E. degree in mechanical engineering from the University of Pune, Pune, India, in 2004, and the Ph.D. degree in high-voltage engineering from the Chalmers University of Technology, Gothenburg, Sweden, in 2017.

Since 2017, he has been with the ABB Technology Center, Skien, Norway, where he is currently a Research and Development Team manager. His current research interests include the development of first principle methods for simulating the behavior of insulating media, plasma physics, fluid transport and structural dynamica.

Sergio Barrio received the M.Sc. degree in Industial Engineering from the University School of Engineering of Bilbao, Spain, in 2005.

His employment experience includes Product Engineer in ACE Group and R&D Product Engineer in Gestamp Automotive. From 2012, he has been working in Ormazabal Corporate Technology as a Research Engineer. He combines tasks of engineering design of switchgear components and systems with “virtual” verification by finite element technology.

Jaroslav Snaidr received the M.Sc. and Ph.D. degrees in electrical power engineering from the University of West Bohemia, Pilsen, Czech Republic in 2011 and 2016 respectively.

Since 2014, he has been with Schneider Electric Sachsenwerk, Regensburg, Germany, where he is currently Principal Technical Expert. His research interests include temperature rise, internal arc, short-time current and dielectric analysis and development of virtual validation methods in medium voltage switchgear industry.

ZuHui Li received the M.Sc. degree in mechanical engineering from Zhejiang University in Hangzhou, China in 2006.

Since 2008 he has been with Eaton Electric Ltd where he is currently working as Simulation Group Leader.

His current research interests are on modeling and simulation in electrical product, include thermal, magnetic, dielectric, structure, dynamic, arc simulation and multi-physics coupling simulation.